

© 2020 IEEE. Personal use of this material is permitted. Permission from IEEE must be obtained for all other uses, in any current or future media, including reprinting/republishing this material for advertising or promotional purposes, creating new collective works, for resale or redistribution to servers or lists, or reuse of any copyrighted component of this work in other works.

# Parameter Estimation and Weighted Signal Optimization for Joint Communication and Radar Sensing

Zhitong Ni<sup>1,2</sup>, J. Andrew Zhang<sup>1</sup>, Xiaojing Huang<sup>1</sup>, Kai Yang<sup>2</sup>, and Fei Gao<sup>2</sup>

<sup>1</sup> University of Technology Sydney, Global Big Data Technologies Centre (GBDTC), Australia

<sup>2</sup> Beijing Institute of Technology, School of Information and Electronics, China  
zhitong.ni@student.uts.edu.cn; Andrew.Zhang@uts.edu.au; yangkai@bit.edu.cn.

**Abstract**—Joint communication and radar sensing (JCAS) integrates communication and radio sensing into one system, sharing one transmitted signal. In this paper, we study a JCAS system that uses a dedicated low-cost single-antenna receiver for sensing. We provide sensing parameter estimation algorithms for the JCAS system, and investigate the optimization of precoding matrix to balance communication and sensing performance. A MUSIC-based estimation approach is proposed to obtain time delays and angle-of-arrivals of targets. A weighted signal optimization to balance between communication and sensing is then provided. Numerical results are provided and verify the effectiveness of the proposed scheme.

**Index Terms**—Joint communication and radar sensing, mobile networks, radar-communications

## I. INTRODUCTION

Sharing many commonalities in terms of hardware, signal processing and system architecture, wireless communication and radar sensing are likely to be integrated in one system using joint communication and radar sensing (JCAS) technologies [1–6]. JCAS can not only reduce cost and size of the system by using one set of hardware component, but also save spectrum resources by transmitting communication and radar sensing signals in the same frequency band.

Some papers [7–12] adopted convex optimization techniques to optimize the JCAS waveforms. In [7], the authors jointly designed radar beamforming (BF) vector and communication covariance matrix to maximize the radar SINR with a given specific capacity. The work in [8, 9] further introduced a sub-sampling matrix for radar as an objective function of optimization. The authors in [10] proposed a robust BF for the base station (BS) and maximized the radar detection probability with a given SINR requirements. In [11], the authors exploited multi-user interference (MUI) as a source of transmitting

power and proposed a novel communication and radar spectrum sharing (CRSS) BF that saves the transmission energy at BS significantly compared to conventional methods. In [12], the authors proposed to split the antennas into two groups for radar and communication separately. The separated design makes the radar signal fall into the null space of downlink channel. These designs, however, all considered the scenario of narrowband systems. The orthogonal frequency division multiplexing (OFDM) signal model has been seen as an possible way to transmit high data rate in terms of vehicle-to-vehicle (V2V) communication and other communication standards such as WiFi.

Wideband JCAS systems based on OFDM can potentially achieve higher resolution compared with narrowband systems. Sturm et al. [1] developed an OFDM-based element-wise division technique to obtain the channel state information (CSI) and then used a discrete Fourier transform (DFT) to estimate the range and Doppler shift of targets independently. The scheme requires a pair matching method and a large number of subcarriers to obtain the estimates. In the scenario of multiuser systems, Sturm et al. [13] proposed an interleaved OFDM signal model in order to mitigate the MUI. Each user is allocated with a non-overlapping set of subcarriers. This design, however, decreases the sum rate of communication, since each user occupies a unique frequency band. The authors in [14] analyzed the MUI tolerance of a MIMO-OFDM based JCAS system in terms of the resulting radar SINR, with using the signal model presented in [13].

In this paper, we study sensing parameter estimation and transmission waveform optimization problem in a JCAS system that uses a dedicated low-cost single-antenna receiver for sensing. To enable using the reflected transmitted signals for sensing, the transceiver needs the capability to work in a full-duplex mode, which is

technically challenging at the moment. To resolve this problem, we consider a single-antenna receiver that is co-located with a large antenna array at the BS and dedicated for sensing the targets by using the downlink communication signals. We first show that how the major sensing parameters can be effectively estimated using the single-antenna receiver. Specifically, the angle-of-departure (AoD) can be equivalently used to locate the angle of arrival (AoA) of targets, due to the co-located architecture. We show that both AoDs and delays can be estimated using a MUSIC algorithm. Then, we propose a joint waveform optimization approach that can be applied to balance the desired sensing and communication performance. The joint optimization problem is formulated as a constrained non-convex problem, and an iterative method is proposed to solve this problem.

Notations:  $\mathbf{a}$  denotes a vector,  $\mathbf{A}$  denotes a matrix, italic English letters like  $N$  and lower-case Greek letters  $\alpha$  are a scalar,  $\angle a$  is the phase angle of complex value  $a$ .  $|\mathbf{A}|$ ,  $\mathbf{A}^T$ ,  $\mathbf{A}^*$ ,  $\mathbf{A}^\dagger$  represent determinant value, transpose, conjugate transpose, pseudo inverse respectively. We denote Frobenius norm of a matrix as  $\|\mathbf{A}\|_F$ . We use  $\text{diag}(\alpha_1, \dots, \alpha_k)$  to denote a diagonal matrix.  $[\mathbf{A}]_N$  is the  $N$ th column of a matrix.

## II. SYSTEM AND CHANNEL MODELS

We consider a JCAS network, consisting of a BS and multiple mobile users (MUs), with adopting the downlink sensing model as proposed in [6]. The BS is equipped with a normal uniform linear array (ULA) for communications, and each MU has a single antenna. To enable the use of the reflected downlink signal from BS for sensing, the BS also uses another receiver with a single antenna, which is sufficiently separated from the ULA to suppress leaked transmit signal. This receiver is synchronized to the transmitted signals of ULA and dedicated for sensing. Since it is only a single-antenna device, the incurred additional cost is insignificant.

The transmitted signal bandwidth, which is used for both communication and sensing, consists of  $K$  orthogonal subcarriers with the subcarrier interval being  $\Delta f = 1/T$ , where  $T$  denotes the time length of one OFDM symbol. Each OFDM symbol is appended with a cyclic prefix (CP) of length  $T_C$  to remove the inter-symbol interference (ISI) caused by frequency-selective wireless channels. The length of CP is selected as the maximum propagation delay in both communication and sensing channels. Assuming that the BS sends  $M$  continuous OFDM symbols, and the  $m$ th OFDM symbol

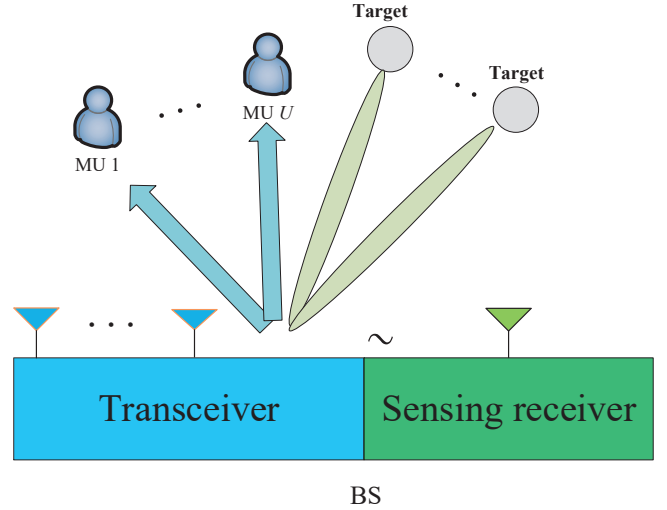


Fig. 1. JCAS system with downlink sensing. The BS uses a single-antenna receiver dedicated for sensing the reflected downlink signals.

is given by

$$\mathbf{x}(m) = \sum_{k=0}^{K-1} \mathbf{s}[k, m] \exp(j2\pi k \Delta f m T_A), \quad (1)$$

where  $\mathbf{s}[k]$  denotes an  $N \times 1$  waveform vector transmitted on the  $k$ th subcarrier, and  $T_A = T + T_C$  denotes the length of an OFDM symbol with including the CP.

For the propagation channels of sensing, the transmitted signal impinges on  $G$  moving targets with the relative velocity of  $\{v_g\}_{g=1}^G$  and the distance of  $\{R_g\}_{g=1}^G$ . The reflected signal after removing the CP is then transformed into digital domain using the sampling frequency of  $K/T$ . By conducting  $K$ -point FFT's on the digital signals, we can obtain the reflected signals at each subcarrier of the  $m$ th OFDM symbol as [13–15]

$$\begin{aligned} & y[k, m] \\ &= \sum_{g=1}^G \beta_g \mathbf{a}_g^* \exp\left(-j2\pi k \frac{\tau_g}{T}\right) \mathbf{s}[k, m] \exp(j2\pi f_{D,g} m T_A) \\ & \quad + n[k, m] \\ &= \mathbf{g}^*[k] \mathbf{s}[k, m] \exp(j2\pi f_{D,g} m T_A) + n[k, m], \end{aligned} \quad (2)$$

where  $\beta_g$  denotes the attenuation caused by path loss and reflection of the  $g$ th target,  $\mathbf{a}_g$  is an  $N \times 1$  array response vector of ULA,  $\tau_g = 2R_g/c_0$  is the time delay with  $c_0$  being the speed of light,  $f_{D,g} = 2f_c v_g/c_0$  is the Doppler frequency offset with  $f_c$  being the carrier frequency,  $n[k, m]$  is a complex additive-white-Gaussian noise (AWGN) at receiver of BS with zero mean and variance of  $\sigma_1^2$ , and  $\mathbf{g}[k]$  denotes the radar channel at frequency domain. We assume a line-of-sight (LoS) path from the BS to each target, i.e.,  $\mathbf{a}_g = \mathbf{a}(\theta_g)$ , with  $\theta_g$

being AoDs.

Meanwhile, the transmit array communicates with  $U$  MUs. The received signal at each MU is

$$r_u[k, m] = \mathbf{h}_u^*[k, m]\mathbf{s}[k, m] + n'_u[k, m], \quad (3)$$

where  $\mathbf{h}_u[k, m]$  is the channel matrix between BS and MU at subcarrier  $k$ , and  $n'_u[k, m]$  is a complex AWGN noise of MU  $u$  with zero mean and variance of  $\sigma_2^2$ . For MUs, we also assume a LoS path. Our proposed waveform design has no particular requirement for the expression of both  $\mathbf{g}[k]$  and  $\mathbf{h}_u[k, m]$ .

### III. SENSING PARAMETER ESTIMATION

In this section, we illustrate how to estimate the major sensing parameters, delay, AoA and Doppler frequency.

We assume that Doppler phase shift is approximately invariant during a short period from  $m = 1$  to  $m = M_0 \geq N$  OFDM symbols. The data symbols of total  $M_0$  OFDM symbols with neglecting the impact of Doppler shift are denoted as  $\mathbf{s}[k]$ , which can be either the training sequence or the precoded data symbols. The received signal block from  $m = 1$  to  $m = M_0$  is written as

$$\begin{aligned} \mathbf{y}^*[k] &\approx \sum_{g=1}^G \beta_g \exp\left(-j2\pi k \frac{\tau_g}{T}\right) \mathbf{a}_g^* \mathbf{s}[k] + \mathbf{n}^*[k] \\ &= \mathbf{e}^*[k] \mathbf{B}^* \mathbf{A}^* \mathbf{s}[k] + \mathbf{n}^*[k] \\ &= \mathbf{g}^*[k] \mathbf{s}[k] + \mathbf{n}^*[k], \end{aligned} \quad (4)$$

where  $\mathbf{e}[k]$  is a  $G \times 1$  vector with the  $g$ th entry being  $\exp(j2\pi k \frac{\tau_g}{T})$ ,  $\mathbf{B} = \text{diag}(\beta_1, \dots, \beta_G)$  with  $\beta_g$  being the path loss of the  $g$ th target,  $\mathbf{A} = [\mathbf{a}_1, \dots, \mathbf{a}_G]$  is the array response matrix, and  $\mathbf{n}[k]$  is a complex AWGN noise vector.

We use traditional MMSE estimation to obtain  $\hat{\mathbf{g}}[k]$ , i.e.,  $\hat{\mathbf{g}}[k] = \mathbf{y}^*[k](\mathbf{S}^*[k])(\mathbf{S}[k]\mathbf{S}^*[k] + \frac{\sigma_1^2}{P}\mathbf{I}_N)^{-1}$ . After obtaining  $\hat{\mathbf{g}}[k]$ , we stack  $\hat{\mathbf{g}}[k]$  from  $k = 0$  to  $k = K - 1$  into a  $K \times N$  matrix, i.e.,

$$\begin{aligned} \mathbf{\Gamma} &= [\hat{\mathbf{g}}[0], \dots, \hat{\mathbf{g}}[K-1]]^* \\ &\approx [\mathbf{e}[0], \mathbf{e}[1], \dots, \mathbf{e}[K-1]]^* \mathbf{B}^* \mathbf{A}^* \\ &\triangleq [\mathbf{c}_1, \dots, \mathbf{c}_G] \mathbf{B}^* \mathbf{A}^*, \end{aligned} \quad (5)$$

where  $\mathbf{c}_g$  equals  $\exp(j2\pi\tau_g(0, 1, \dots, K-1))^T$ . We let the singular value decomposition (SVD) of  $\mathbf{\Gamma}$  be

$$\mathbf{\Gamma} = \mathbf{U}_\Gamma \mathbf{E}_\Gamma \mathbf{V}_\Gamma^*, \quad (6)$$

where  $\mathbf{U}_\Gamma$  is the left signal matrix with the dimension of  $K \times G$  and  $\mathbf{V}_\Gamma$  is the right singular matrix with the dimension of  $N \times G$ . It is noted that  $\mathbf{U}_\Gamma$  can be seen as a subspace spanned by  $G$  vectors that are related to delays. In the same way,  $\mathbf{V}_\Gamma$  can be seen as a subspace

that is related to  $G$  AoDs. Denote the null-space of  $\mathbf{U}_\Gamma$  and the null-space of  $\mathbf{V}$  as  $\bar{\mathbf{U}}_\Gamma$  and  $\bar{\mathbf{V}}_\Gamma$ , respectively, the time delays and AoDs can be obtained via MUSIC

$$\hat{\tau}_g = \arg \max_{\tau_g} \frac{1}{\|\mathbf{e}_g^* \bar{\mathbf{U}}_\Gamma\|_F^2}. \quad (7)$$

In the same way, AoDs can also be estimated by (7) with  $\mathbf{e}_g$  replaced by  $\mathbf{a}_g$  and  $\bar{\mathbf{U}}_\Gamma$  replaced by  $\bar{\mathbf{V}}_\Gamma$ .

### IV. WEIGHTED SIGNAL OPTIMIZATION FOR JCAS

In this section, we aim to optimize the waveforms for JCAS systems, taking into consideration of the sensing parameter estimation in Section III. We consider to implement a digital precoder, i.e.,

$$\mathbf{s}[k] = \mathbf{P}[k]\mathbf{b}[k], \quad (8)$$

where  $\mathbf{b}[k]$  is a  $U \times 1$  vector and  $\mathbf{P}[k]$  is an  $N \times U$  precoder that precodes  $\mathbf{b}[k]$  in the frequency domain.  $\mathbf{P}[k]$  will be optimized for achieving both SDMA communications and sensing.

For radar sensing, note that we can first use the non-precoded training sequence to get some initial estimation for some sensing parameters, in particular, the delay and AoAs. Therefore, the precoding is optimized for signals containing data symbols that will be further used for improving the sensing performance. With the availability of the initial estimate of  $\mathbf{A}$ , we aim to maximize the combining gain of targets as

$$\tilde{I} = \sum_{k=0}^{K-1} \|\mathbf{A}^* \mathbf{P}[k]\|_F^2, \quad (9)$$

where  $\tilde{I}$  denotes the sum of the projected length of each precoding vector into the subspace of  $\mathbf{A}$ .

For communications, we consider the MUI, which is the power leakage from other users, i.e.,

$$\begin{aligned} \text{MUI} &= \sum_{k=1}^K \sum_{u=1}^U |\mathbf{h}_u^*[k] \mathbf{P}[k] \mathbf{s}[k] - s_u[k]|^2 \\ &\leq \sum_{k=1}^K \|\mathbf{H}^*[k] \mathbf{P}[k] - \mathbf{E}\|_F^2 \\ &\triangleq \tilde{J}, \end{aligned} \quad (10)$$

where  $\mathbf{H}[k] = [\mathbf{h}_1[k], \dots, \mathbf{h}_U[k]]$  denotes the channel matrix of all MUs,  $s_u$  is the  $u$ th data symbol, and  $\mathbf{E}$  is a diagonal matrix with the  $u$ th entry being  $s_u^2$ . Assuming that  $\mathbf{E}$  is a scaled identity matrix, the optimal precoder that minimizes the MUI is  $\mathbf{P}[k] = (\mathbf{H}^*[k])^\dagger$ .

We intend to jointly consider both problems of maximizing  $\tilde{I}$  and minimizing  $\tilde{J}$ . Directly using weighted sum of two individual problems is inappropriate, hence we

change the sign of maximizing  $\tilde{I}$  and provide a weighted sum problem of minimizing  $\tilde{J}$  and  $-\tilde{I}$ , i.e.,

$$\begin{aligned} \arg \min_{\mathbf{P}[k]} f(\mathbf{P}[k]) &= \mu\tilde{J} - (1 - \mu)\tilde{I} \\ \text{s.t. } \|\mathbf{P}[k]\|_F^2 &\leq P, \end{aligned} \quad (11)$$

where  $P$  is the power constraint at each subcarrier. The objective function in (11) becomes a non-convex function due to the change of sign. Due to the quadratic form of  $f(\mathbf{P}[k])$ , we propose a novel approach to solve the non-convex joint function in (11).

For notational simplicity, we assume  $K = 1$  and omit the parameter  $k$ . The joint function is rewritten as

$$\begin{aligned} f(\mathbf{P}) &= \mu \text{tr}(\mathbf{P}^* \mathbf{H} \mathbf{H}^* \mathbf{P} - \mathbf{E} \mathbf{H}^* \mathbf{P} - \mathbf{P}^* \mathbf{H} \mathbf{E} + \mathbf{E}^2) \\ &\quad - (1 - \mu) \text{tr}(\mathbf{P}^* \mathbf{U} \mathbf{U}^* \mathbf{P}) \\ &= \text{tr}(\mathbf{P}^* (\mu \mathbf{C}_H - (1 - \mu) \mathbf{C}_A) \mathbf{P}) \\ &\quad - \mu \text{tr}(\mathbf{E} \mathbf{H}^* \mathbf{P} + \mathbf{P}^* \mathbf{H} \mathbf{E} - \mathbf{E}^2) \\ &= \sum_{u=1}^U \mathbf{p}_u^* (\mu \mathbf{C}_H - (1 - \mu) \mathbf{C}_A) \mathbf{p}_u \\ &\quad - \mu e_u (\mathbf{h}_u^* \mathbf{p}_u + \mathbf{p}_u^* \mathbf{h}_u - e_u) \\ &\triangleq \sum_{u=1}^U \mathbf{p}_u^* \mathbf{C} \mathbf{p}_u - \mu e_u (\mathbf{h}_u^* \mathbf{p}_u + \mathbf{p}_u^* \mathbf{h}_u - e_u), \end{aligned} \quad (12)$$

where  $\mathbf{p}_u$  is the  $u$ th vector of  $\mathbf{P}$ ,  $\mathbf{C}_A = \mathbf{A} \mathbf{A}^*$  and  $\mathbf{C}_H = \mathbf{H} \mathbf{H}^*$  denote correlation matrices of  $\mathbf{U}$  and  $\mathbf{H}$ , respectively, and  $\mathbf{C} = \mu \mathbf{C}_H - (1 - \mu) \mathbf{C}_A$ . Note that  $\mathbf{C}$  is not a semi-definite matrix and makes the problem hard to solve. We take SVD of  $\mathbf{C}$  as

$$\mathbf{C} = \mathbf{V} \mathbf{\Lambda} \mathbf{V}^*, \quad (13)$$

where  $\mathbf{\Lambda}$  is a diagonal full-rank matrix and  $\mathbf{V}$  is a unitary matrix. Since we let the left singular matrix and the right singular matrix to be the same, the diagonal entries of  $\mathbf{\Lambda}$  may be negative. Letting

$$\mathbf{p}_u = \mathbf{V} (\mathbf{q}_u + \mu e_u \mathbf{\Lambda}^{-1} \mathbf{V}^* \mathbf{h}_u) \quad (14)$$

where  $\mathbf{q}_u$  is a  $L \times 1$  vector with  $L = \text{rank}(\mathbf{C})$ . Substituting  $\mathbf{p}_u$  into (12), we transform the joint optimization problem into

$$\begin{aligned} \arg \min_{\mathbf{q}_u} f(\mathbf{q}_u) &= \sum_{u=1}^U (\mathbf{q}_u^* \mathbf{\Lambda} \mathbf{q}_u) \\ \text{s.t. } \sum_{u=1}^U \|\mathbf{q}_u + \mu e_u \mathbf{\Lambda}^{-1} \mathbf{V}^* \mathbf{h}_u\|_F^2 &\leq P. \end{aligned} \quad (15)$$

We note that  $\mathbf{\Lambda}$  has both negative and positive diagonal entries, hence  $f(\mathbf{q}_u)$  is still a non-convex function. More specifically,  $f(\mathbf{q}_u)$  is a saddle surface. The constraint is a complex sphere with the sphere center being

$$-\mu e_u \mathbf{\Lambda}^{-1} \mathbf{V}^* \mathbf{h}_u.$$

We prove that the optimal points that minimizes (15) are obtained by letting the curve of  $g(\mathbf{q}_u) = \sum_{u=1}^U \|\mathbf{q}_u + \mu e_u \mathbf{\Lambda}^{-1} \mathbf{V}^* \mathbf{h}_u\|_F^2 = P$  and the curve of  $f(\mathbf{q}_u) = f_0$  be tangent.

*Proof:* In (15), each element of  $\mathbf{q}_u$  is independent of each other. Supposed that the  $j$ th diagonal entry of  $\mathbf{\Lambda}$  is negative, and given an arbitrary point of  $\mathbf{q}_u$  satisfying  $g(\mathbf{q}_u) < P$ , it is easy to find a new  $[\mathbf{q}_u]_j$  that has a larger modulus than its original value, such that  $g(\mathbf{q}_u) = P$ . Noting that  $f(\mathbf{q}_u) = \mathbf{q}_u^* \mathbf{\Lambda} \mathbf{q}_u$ , the larger modulus of  $[\mathbf{q}_u]_j$  means the smaller  $f(\mathbf{q}_u)$ . Therefore, the minimal value of  $f(\mathbf{q}_u)$  is on the surface of  $g(\mathbf{q}_u) = P$ . Similarly, the maximal value is also on the surface of  $g(\mathbf{q}_u) = P$ .

Given  $f(\mathbf{q}_u) = f_0$ , which is the surface that makes  $f(\mathbf{q}_u)$  reach its globally minimum value, this curve cannot be intersected with  $g(\mathbf{q}_u) = P$ . Otherwise, the inner point of  $g(\mathbf{p}_u) = P$  also minimizes  $f(\mathbf{q}_u)$ . Therefore, the minimal value of  $f(\mathbf{q}_u)$  is reached when  $f(\mathbf{q}_u) = f_0$  and  $g(\mathbf{q}_u) = P$  are tangent. ■

We obtain the tangent plane of  $g(\mathbf{q}_u) = P$  as

$$\begin{aligned} &\left( \frac{\partial g}{\partial \mathbf{q}_u} \bigg|_{\mathbf{q}_u = \mathbf{q}_u^0} \right)^* (\mathbf{q}_u - \mathbf{q}_u^0) \\ &= 2(\mathbf{q}_u^0 + \mu e_u \mathbf{\Lambda}^{-1} \mathbf{V}^* \mathbf{h}_u)^* (\mathbf{q}_u - \mathbf{q}_u^0) = 0, \end{aligned} \quad (16)$$

where  $\mathbf{q}_u^0$  is the tangent point, and we obtain the tangent plane of  $f(\mathbf{p}_u)$  as

$$\begin{aligned} &\left( \frac{\partial f}{\partial \mathbf{q}_u} \bigg|_{\mathbf{q}_u = \mathbf{q}_u^0} \right)^* (\mathbf{q}_u - \mathbf{q}_u^0) \\ &= (2\mathbf{\Lambda} \mathbf{q}_u^0)^* (\mathbf{q}_u - \mathbf{q}_u^0) = 0. \end{aligned} \quad (17)$$

Since the curve of  $f(\mathbf{q}_u) = f_0$  is tangent with  $g(\mathbf{q}_u) = P$ , the plane of (16) and (17) are the same. Hence, the optimal  $\mathbf{q}_u$  satisfies that

$$\begin{cases} \mathbf{q}_u + \mu e_u \mathbf{\Lambda}^{-1} \mathbf{V}^* \mathbf{h}_u = \lambda \mathbf{\Lambda} \mathbf{q}_u \\ \sum_{u=1}^U \|\mathbf{q}_u + \mu e_u \mathbf{\Lambda}^{-1} \mathbf{V}^* \mathbf{h}_u\|_F^2 = P \end{cases}, \quad (18)$$

where  $\lambda$  is an unknown factor that is not zero. The value of  $\lambda$  depends on  $P$ . With a given  $P$ , (18) generates a  $2U$ th order equation of  $\lambda$ , denoting the cases of inner-tangent plane and outer-tangent plane. It is noted that the closed-form solution of  $\lambda$  is unable to obtain when  $U$  is too large, e.g., 2.

Next, we propose an iterative algorithm that makes  $\lambda$  infinitely approach to the closed-form solution. To avoid  $f(\mathbf{q}_u)$  reaching the maximum point, we assume  $P$  is sufficiently large and take an initial point of  $\mathbf{q}_u$ , denoted as  $\mathbf{q}_u^{(0)}$ , such that  $g(\mathbf{q}_u^{(0)}) = P$  and  $f(\mathbf{q}_u^{(0)}) < 0$ .

---

**Algorithm 1** Iterative Weighted Sum Optimal Precoder Design
 

---

- 1: **Input:**  $\mathbf{A}$  and  $\mathbf{H}[k]$ .
  - 2: **Initialization:** Determine  $\delta$ ,  $\mu$ ,  $P$ , and  $\mathbf{E} = \text{diag}(e_1, \dots, e_U)$ . Iteration index is  $i = 0$ . The objective function is denoted as  $f(\mathbf{q}_u)$ .
  - 3: Generate  $\mathbf{C}[k] = \mu\mathbf{H}[k]\mathbf{H}^*[k] - (1 - \mu)\mathbf{A}\mathbf{A}^*$ .
  - 4: Take the SVD of  $\mathbf{C}[k]$ ,  $\mathbf{C}[k] = \mathbf{V}[k]\mathbf{\Lambda}[k]\mathbf{V}^*[k]$ .
  - 5: Find an initial point of  $\mathbf{q}_u^{(0)}[k]$ , such that (1):  $g(\mathbf{q}_u) = P$ ; (2):  $\mathbf{q}_u^*[k]\mathbf{\Lambda}[k]\mathbf{q}_u[k] < 0$ .
  - 6: **while**  $\|\mathbf{q}_u^{(i)}[k] - \mathbf{q}_u^{(i-1)}[k]\|_F^2 > \delta$  **do**
  - 7: Choose one out of two temporary points expressed as (19), such that  $f(\bar{\mathbf{q}}_u^{(i)}[k]) < f(\mathbf{q}_u^{(i)}[k])$ .
  - 8: Generate  $\mathbf{q}_u^{(i+1)}[k]$  according to (20).
  - 9:  $i = i + 1$ .
  - 10: **end while**
  - 11: **Output:**  $\mathbf{p}_u^*[k] = \mathbf{V}[k](\mathbf{q}_u^{(i)}[k] + \mu e_u \mathbf{\Lambda}^{-1}[k]\mathbf{V}^*[k]\mathbf{h}_u[k])$ .
- 

We make a small step of length  $\varepsilon > 0$  from  $\mathbf{q}_u^{(i)}$  to generate two temporary points, which are written as

$$\begin{aligned} \bar{\mathbf{q}}_{u+}^{(i)} &= \mathbf{q}_u^{(i)} + \frac{\partial f}{\partial \mathbf{q}_u} \varepsilon \\ \bar{\mathbf{q}}_{u-}^{(i)} &= \mathbf{q}_u^{(i)} - \frac{\partial f}{\partial \mathbf{q}_u} \varepsilon. \end{aligned} \quad (19)$$

Aiming to make  $f(\bar{\mathbf{q}}_u^{(i)}) < f(\mathbf{q}_u^{(i)})$ , we denote the one with smaller  $f$  as  $\bar{\mathbf{q}}_u^{(i)}$ . Then, we project  $\bar{\mathbf{q}}_u^{(i)}$  into the surface of  $g(\mathbf{q}_u) = P$  to generate the next iterative point. The projective point has the minimum distance with  $\bar{\mathbf{q}}_u^{(i)}$ . It is noted that the surface of  $g(\mathbf{q}_u) = P$  is a sphere with center being  $-\mu e_u \mathbf{\Lambda}^{-1} \mathbf{V}^* \mathbf{h}_u$ . Hence, the projective point is given by

$$\mathbf{q}_u^{(i+1)} = a \bar{\mathbf{q}}_u^{(i)} + (a - 1)(\mu e_u \mathbf{\Lambda}^{-1} \mathbf{V}^* \mathbf{h}_u), a > 0, \quad (20)$$

where  $a$  is a real value, such that  $g(\mathbf{q}_u^{(i+1)}) = P$ .

With the number of iterations increasing,  $f(\bar{\mathbf{q}}_u^{(i)})$  drops. The new iterative point infinitely approaches to the tangent point. The iteration can be terminated when  $\|\mathbf{q}_u^{(i)} - \mathbf{q}_u^{(i-1)}\|_F^2 \leq \delta$  with  $\delta$  being a threshold that denotes the error between the final iterative point and the tangent point.

The proposed iterative optimization approach is summarized in Algorithm 1 for any subcarrier  $k$ .

## V. SIMULATION RESULTS

In this section, we provide simulation results to validate the proposed scheme, following the system and channel models introduced in Section II. We simulate

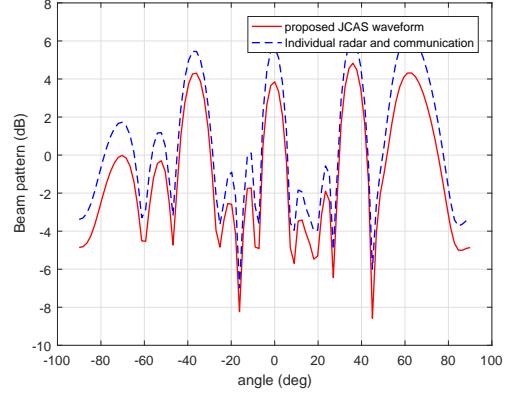


Fig. 2. Beam patterns with employing individual and joint designs.

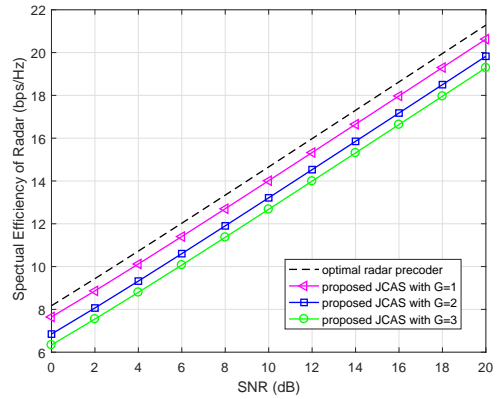


Fig. 3. Spectral Efficiency versus SNR for radar targets with employing individual and joint designs.

a scenario where a BS communicates with  $U = 2$  MUs and detects  $G = 2$  targets. The BS adopts a  $16 \times 1$  ULA as the transmit antennas, uses BPSK to transmit a  $3 \times 1$  data symbol vector on each subcarrier. The number of subcarriers is  $K = 256$ . The AoDs that are uniformly distributed from  $-\pi$  to  $\pi$ . The delay of each target is a random value ranging from 0 to  $T/2 = 0.5$  ms. One OFDM symbol has a length of  $T_A = 1.5$  ms. The weighted factor is  $\mu = 0.5$ .

Fig. 2 illustrates an example of beam patterns for different designs. For individual design, which is a combination of individual optimal radar and communication precoders, i.e.,  $\mathbf{P}[k] = [\mathbf{A}, (\mathbf{H}^*[k])^\dagger]$ , we see that there are four main lobes located at  $-35^\circ, 0^\circ, 35^\circ$ , and  $60^\circ$ , which indicate the AoDs of targets and MUs. Our proposed precoder matches with the individual design tightly. However, it is noted that the individual precoder needs four RF chains for communication and radar sensing in total while our proposed JCAS precoder only needs  $U = 2$  RF chains.

Fig. 3 unfolds the achieved spectral efficiency (SE) of

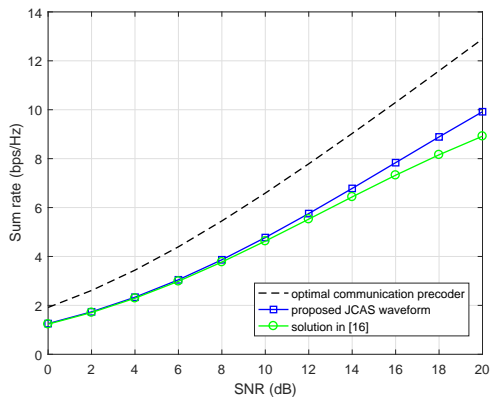


Fig. 4. Sum rate of multiple MUs versus SNR for communications.

radar with using the JCAS precoder, i.e.,

$$S = \frac{1}{K} \sum_{k=1}^K \log_2 |\mathbf{I}_U + \mathbf{P}^*[k]\mathbf{g}[k]\mathbf{g}^*[k]\mathbf{P}[k]|, \quad (21)$$

where  $\mathbf{I}_U$  is a  $U \times U$  identity matrix. We see that the SE increases linearly with SNR increasing. The SE achieved by the optimal radar precoder,  $\mathbf{P}[k] = \mathbf{A}$ , remains the highest. Our proposed precoder achieves a satisfactory SE and approaches to that of the individual optimal precoder with  $G$  decreasing. This can be explained by the fact that, with  $G$  decreasing, the precoder has less distortion between the individual radar precoder and the JCAS precoder.

Fig. 4 shows how the sum rate of multiple users varies with SNRs using different designs. For the precoder optimized solely for communication, its sum rate remains the highest. Our proposed precoder achieves better performance than the solution in [16], which is mainly because our proposed algorithm maximizes the spectral efficiency and minimizes MUI for MUs simultaneously, while the weighted solution needs to determine a desired constellation symbol matrix.

## VI. CONCLUSION

In this paper, we studied the sensing parameter estimation and transmission waveform optimization problem for a JCAS system using a dedicated single-antenna receiver for sensing. We provided a closed-form solution to the joint optimization problem and proposed an iterative algorithm to obtain the optimal precoder. The beam pattern of our proposed solution matches with the individual optimal solution tightly. The achieved spectral efficiency of sensing approaches to the individual design with the number of targets decreasing. The achieved sum rate for communications outperforms the existing solution.

## REFERENCES

- [1] C. Sturm and W. Wiesbeck, "Waveform design and signal processing aspects for fusion of wireless communications and radar sensing," *Proc. IEEE*, vol. 99, pp. 1236–1259, Jul. 2011.
- [2] A. R. Chiriyath, B. Paul, and D. W. Bliss, "Radar-communications convergence: Coexistence, cooperation, and co-design," *IEEE Trans. on Cogn. Commun. Netw.*, vol. 3, pp. 1–12, Mar. 2017.
- [3] J. A. Zhang, X. Huang, Y. J. Guo, J. Yuan, and R. W. Heath, "Multibeam for joint communication and radar sensing using steerable analog antenna arrays," *IEEE Trans. Veh. Technol.*, vol. 68, pp. 671–685, Jan. 2019.
- [4] Y. Luo, J. A. Zhang, X. Huang, W. Ni, and J. Pan, "Optimization and quantization of multibeam beamforming vector for joint communication and radio sensing," *IEEE Trans. Commun.*, vol. 67, pp. 6468–6482, Sep. 2019.
- [5] P. Kumari, J. Choi, N. Gonzalez-Prelcic, and R. W. Heath, "IEEE 802.11ad-based radar: An approach to joint vehicular communication-radar system," *IEEE Trans. Veh. Technol.*, vol. 67, pp. 3012–3027, Apr. 2018.
- [6] M. L. Rahman, J. A. Zhang, X. Huang, Y. J. Guo, and R. W. Heath Jr, "Framework for a perceptive mobile network using joint communication and radar sensing," *IEEE Transactions on Aerospace and Electronic Systems*, pp. 1–1, 2019.
- [7] B. Li and A. Petropulu, "Mimo radar and communication spectrum sharing with clutter mitigation," in *2016 IEEE Radar Conference (RadarConf)*, pp. 1–6, May 2016.
- [8] B. Li, A. P. Petropulu, and W. Trappe, "Optimum co-design for spectrum sharing between matrix completion based MIMO radars and a MIMO communication system," *IEEE Trans. Signal Process.*, vol. 64, pp. 4562–4575, Sep. 2016.
- [9] B. Li and A. P. Petropulu, "Joint transmit designs for coexistence of MIMO wireless communications and sparse sensing radars in clutter," *IEEE Trans. Aerosp. Electron. Syst.*, vol. 53, pp. 2846–2864, Dec. 2017.
- [10] F. Liu, C. Masouros, A. Li, and T. Ratnarajah, "Robust mimo beamforming for cellular and radar coexistence," *IEEE Wireless Commun. Lett.*, vol. 6, pp. 374–377, Jun. 2017.
- [11] F. Liu, C. Masouros, A. Li, T. Ratnarajah, and J. Zhou, "Mimo radar and cellular coexistence: A power-efficient approach enabled by interference exploitation," *IEEE Trans. Signal Process.*, vol. 66, pp. 3681–3695, Jul. 2018.
- [12] F. Liu, C. Masouros, A. Li, H. Sun, and L. Hanzo, "MU-MIMO communications with MIMO radar: From co-existence to joint transmission," *IEEE Trans. Wireless Commun.*, vol. 17, pp. 2755–2770, Apr. 2018.
- [13] C. Sturm, Y. L. Sit, M. Braun, and T. Zwick, "Spectrally interleaved multi-carrier signals for radar network applications and multi-input multi-output radar," *IET Radar, Sonar Navigation*, vol. 7, pp. 261–269, Mar. 2013.
- [14] Y. L. Sit, B. Nuss, and T. Zwick, "On mutual interference cancellation in a MIMO OFDM multiuser radar-communication network," *IEEE Trans. Veh. Technol.*, vol. 67, pp. 3339–3348, Apr. 2018.
- [15] J. Gu, J. Moghaddasi, and K. Wu, "Delay and doppler shift estimation for ofdm-based radar-radio (radcom) system," in *2015 IEEE International Wireless Symposium (IWS 2015)*, pp. 1–4, Mar. 2015.
- [16] F. Liu, L. Zhou, C. Masouros, A. Li, W. Luo, and A. Petropulu, "Toward dual-functional radar-communication systems: Optimal waveform design," *IEEE Trans. Signal Process.*, vol. 66, pp. 4264–4279, Aug. 2018.